Epitaxial growth of ultra-thin NbN films on $Al_xGa_{1-x}N$ buffer-layers

S. Krause,[1] D. Meledin,[1] V. Desmaris,[1] Alexey Pavolotsky,[1] V. Belitsky,[1] M. Rudziński,[2] and E. Pippel [3]

[1] *Group for Advanced Receiver Development, Chalmers University of Technology,SE-412 96 Gothenburg, Sweden*

[2] *Institute of Electronic Materials Technology (ITME), 01-919 Warsaw, Poland*

[3] *Max Planck Institute of Microstructure Physics, D-06120 Halle/Saale, Germany*

E-mail: sascha.krause@chalmers.se

Abstract: The suitability of $Al_xGa_{1-x}N$ epi-layer to deposit onto ultra-thin NbN films has been demonstrated for the first time. High quality single-crystal films with 5nm thickness confirmed by high-resolution transmission electron microscopy (HRTEM) have been deposited in a reproducible manner by means of reactive DC magnetron sputtering at elevated temperatures and exhibit critical temperatures (Tc) as high as 13.2K and residual resistivity ratio (RRR)~1 on hexagonal GaN epi-layer. With increasing the Al-content x in the $Al_xGa_{1-x}N$ epi-layer above 20% a gradual deterioration of Tc down to 10K was observed. Deposition of NbN on bare silicon substrates served as reference and comparison. Excellent spatial homogeneity of the fabricated films was confirmed by R(T) measurements of patterned micro-bridges across the entire film area. The superconducting properties of those films were further characterized by critical magnetic field and critical current measurements. It is expected that the employment of GaN material as a buffer-layer for the deposition of ultra-thin NbN films prospectively benefit terahertz electronics, particularly hot electron bolometer (HEB) mixers.

1. Introduction

Hot electron bolometer (HEB) based heterodyne receivers have shown to be the most sensitive detector for spectroscopy in the terahertz frequency range above 1.3 THz [1-3] and are essential for radio astronomical instrumentation [4]. Such phonon-cooled HEB-based mixers widely employ NbN as superconducting material for the bolometers, exploiting short electron-electron and electron-phonon interaction times that yields a decent intermediate frequency (IF) band. The performance of such devices is intrinsically associated with the superconducting properties of the film such as the critical temperature (Tc) at which the phase transition from the resistive to the superconducting state occurs as well as the film thickness [5,6], whereby higher Tc and thinner films are desirable. The challenge of achieving ultimate IF bandwidth is posed by the reduction of Tc from 16-17K of the bulk material and increase in sheet resistance (R_{sheet}) when approaching film thicknesses in the range of a few nanometers [7]. Besides careful optimization of NbN deposition process parameters, the choice of substrate on which to grow NbN is crucial for achieving high Tc and thus high quality 3.5-6nm thin films required for HEBs.

The use of silicon substrate is commonly adopted and features advantageous properties from a processing point of view as well as relatively low losses at THz frequencies. However, due to the significant lattice-mismatch to NbN, only poly-crystalline films, not exceeding a Tc of approximately 10K at 5nm thickness, have been demonstrated [2,8,9]. In order to increase the Tc, hence the

superconducting quality of the NbN ultra-thin films, substrates with low lattice mismatch to NbN such as MgO [10-12], sapphire [13] and the recently demonstrated 3C-SiC have been utilized and provide an epitaxial growth resulting in increased Tc, e.g., 11.8K [14,15]. Processing and life-time issues arise with the use of MgO as a buffer-layer due to its hydrophobic nature and sensitivity to alkaline solutions. Bulk sapphire substrate on the other hand introduce challenges due to its hardness and restrict particularly THz waveguide applications.

Therefore the use of alternative buffer-layers, which could be grown on silicon and still provide a close lattice match to NbN, is the most attractive solution from a perspective of the device fabrication and system integration. The crystallographic orientation of the NbN film does not influence its superconducting properties. As a result, the hexagonal buffer-layers would also be suitable providing that their lattice parameter *a* would match the ones of NbN oriented along its [111] direction. In this paper, we describe the growth of single-crystal ultra-thin NbN films onto hexagonal $Al_xGa_{1-x}N$ substrates by means of reactive DC magnetron sputtering. An extensive characterization of the processed films has been performed including fabrication of micro-bridges, film homogeneity studies, R(T) to study superconducting transition. Furthermore, the crystallographic quality of the films was characterized by high-resolution transmission electron microscopy (HRTEM) and high-angle annular dark field detector/scanning transmission electron microscopy (HAADF/STEM). The results of the NbN/AlGaN compound strongly point towards prospective applications in THz electronics, particularly HEB mixers and circuitry that takes advantage of the enhanced superconducting properties of epitaxially grown NbN films.

2. Experiment

The high-quality 1-2μm thick $Al_xGa_{1-x}N$ wurtzite epi-layers were grown onto 2-inch c-plane sapphire (0001) substrates by metal organic chemical vapor deposition (MOCVD) using a RF heated AIX200/4RF-S low pressure horizontal reactor. The use of sapphire as a substrate on which to grow AlGaN for initial experiments is motivated by its wide availability. In order to validate that the sapphire substrate exerts no influence on the growth of NbN ultra-thin film on AlGaN epi-layer, NbN was also deposited onto the GaN buffer-layer; which was itself grown onto bare silicon substrates.

Samples with different Al content x ranging from 0% (GaN) to 100% (AlN) were prepared and yielded a shift in the lattice constant from $a_{w\text{-}GaN}$=3.189Å to $a_{w\text{-}AlN}$=3.11Å, respectively. It is expected that by changing the Al content, the lattice constant of the cubic δ-NbN phase in its [111]-orientation can be perfectly matched. In addition, AlGaN features lower than Si dielectric constant ε_r, ranging from 8.5-9.5 for AlN and GaN respectively [16], making them applicable in membrane-like structures, i.e. waveguide-based THz applications.

The deposition of NbN ultra-thin films was performed by means of reactive DC magnetron sputtering. The system contains a high-purity 2-inch Nb target and is able to achieve a base pressure of 1.8×10^{-8} mTorr in the process chamber. The substrate holder was pre-heated to either 525°C or 650°C and maintained at this temperature during the sputtering. Furthermore, applied pre-conditioning of the target by excessive sputtering with a closed shutter provided a reliable deposition process. The partial pressure of argon and nitrogen was carefully adjusted and best results were achieved when keeping the ratio N_2/Ar close to 1:9.2 at a fixed DC magnetron current of 0.5A at 2.8mTorr ambient pressure. The deposition rate resulting for these conditions is approximately 1.2Å/s and was deduced from HRTEM and ellipsometry characterizations. Moreover, additional depositions of NbN films on bare silicon wafers with studied superconducting properties were carried out and indicated eventual changes in the quality of the deposition process.

All deposited films were submitted resistance-temperature R(T) measurement in a temperature-calibrated four-point-probe setup. The typical behavior of the resistance as a function of temperature of thin NbN films is illustrated in figure 1. The critical temperature Tc is associated with the transition to the superconducting state and corresponds to a drop of resistance to 50% of its normal-state value, whereas the transition width ΔT is taken from 90% to 10% of the normal-state resistance. A narrow transition width is evidence of high quality structural properties and benefits the sensitivity of e.g. HEBs devices.

The residual resistivity ratio (RRR) is commonly defined as the ratio of film resistance at room temperature and at 20K for NbN.

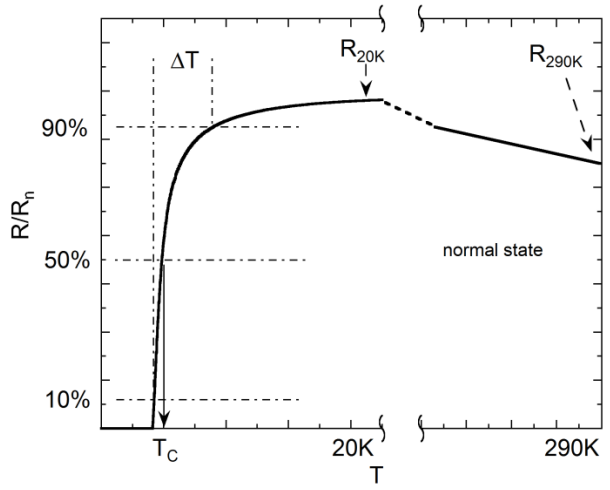

Figure 1. Typical resistance versus temperature behavior of ultra-thin NbN films and indicated figure-of-merit for assessing the quality of the films.

More related to prospective devices is the validation of afore-mentioned properties on a microscopic scale. Thus, micro-bridges with varying bridge dimensions distributed over the entire film area were fabricated, probed and re-measured. From this measurement, the uniformity was deduced by locally assessing the deviation of Tc and R_{sheet}.

Furthermore, critical current and upper critical magnetic field measurements under applied magnetic field ranging from 0 to 15T have been conducted and superconducting parameters, such as zero-field critical current density J_{c0}, second critical magnetic field $\mu_0 H_{c2}$ and the electron diffusion constant D were determined. HRTEM images taken by a TITAN 80-300 accurately verified the fabricated film thickness, whereas HAADF/STEM analysis was employed to assess the interface of NbN and epi-layers as well as revealing crystallographic properties from diffraction patterns obtained by Fourier transform. In the following, the presented HRTEM analysis was conducted on processed micro-bolometers after their comprehensive electrical characterization. The prepared specimen were taken of ultra-thin NbN films deposited on GaN and $Al_{0.54}Ga_{0.46}N$ buffer-layer; which were grown onto sapphire substrates and NbN on bare silicon as comparison.

3. Results and discussion

3.1. NbN on GaN buffer-layer

As seen in figure 2 (a), there is a clear evidence of the epitaxial single-crystal growth of NbN on the GaN buffer in its [111]-orientation. The expected film thickness of 5nm, adequate for application requirements, i.e., HEB mixers, has been confirmed according to the provided scale; the film thickness is reasonably constant across the entire cross-section. Furthermore, the diffraction pattern by taken Fast Fourier Transformation from both NbN and GaN structures coincide and supports the very low lattice-mismatch as illustrated in figure 2 (b). The interface across NbN/GaN exhibits a sharp transition within one atomic layer with very few defects, thus indicating that no inter-diffusion has taken place while depositing at elevated substrate temperatures. Moreover, the high-quality of the NbN/GaN interface may improve the phonon transmissivity [17] and thus particularly benefit the enhancement of phonon-cooled HEB's IF bandwidth.

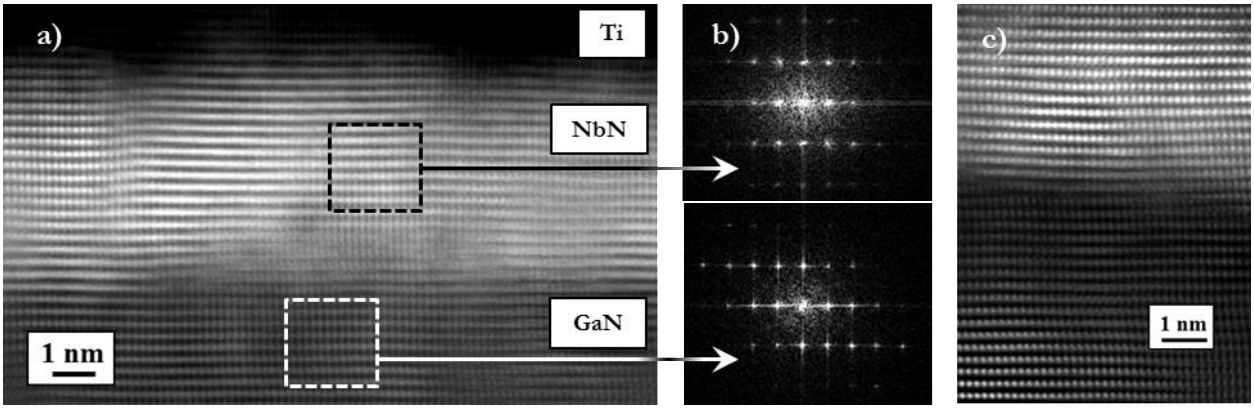

Figure 2. Single-crystal NbN on GaN epi-layer in cross-sectional HAADF/STEM image. (a) Ti/NbN/GaN layer system confirming thickness of approximately 5nm. (b) Diffraction pattern by Fast Fourier Transform (FFT) of selected areas. (c) NbN/GaN interface with no signs of diffusion.

3.2. NbN on AlGaN buffer-layer

In order to study the influence of Al content in the employed $Al_xGa_{1-x}N$ buffer-layers on the quality of NbN films, another specimen with a $NbN/Al_{0.54}Ga_{0.46}N$ compound has been prepared and characterized by HRTEM, HAADF/STEM and FFT. As illustrated in figure 3 (a), the NbN film grown onto AlGaN layer exhibits a mono-crystalline structure with some stacking defects. The film thickness of approximately 5nm is verified across the cross-section. The FFT as shown in figure 3 (b) points to the fact that the lattice-mismatch is slightly increased since the diffraction pattern do not coincide perfectly. Furthermore, it is observed in figure 3 (c) that the AlGaN/NbN interface is not as sharp as that for GaN and features a lower atomic mass indicated in the Z-contrast HAADF/STEM image as a dark region. The origin of this disordered layer is uncertain. We presume that oxidation on the surface has taken place [18], which is more likely to happen with increasing Al content. However, the forming of lighter compounds of Al at elevated substrate temperatures or defects introduced by selective sputter-cleaning are also conceivable.

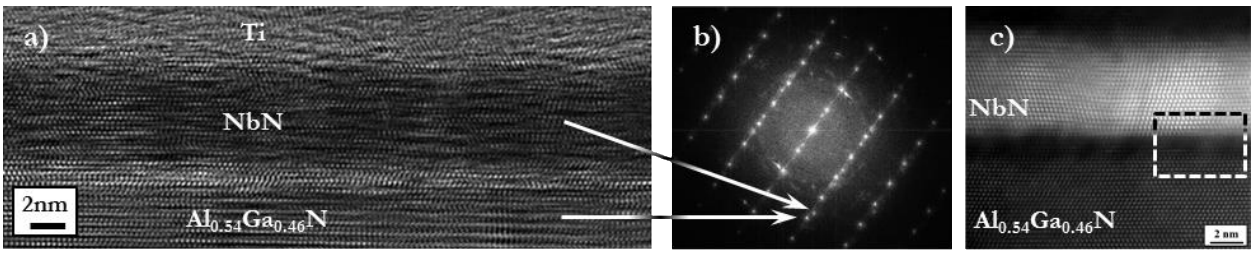

Figure 3. (a) Cross-section of epitaxially grown NbN film on $Al_{0.54}Ga_{0.46}N$ layer in HRTEM image. (b) Superimposed diffraction pattern by FFT taken from AlGaN and NbN. (c) HAADF/STEM reveals lighter and disordered layer across the film/substrate interface as seen as black region.

3.3. NbN on silicon substrate

In comparison to the above presented epitaxially grown films, the cross-section of NbN deposited on bare silicon wafer with native oxide layer of approximately 2nm is depicted in figure 4. The poly-crystalline structure and the arrangement in differently sized grains is clearly visible and contrary to those on GaN and AlGaN samples.

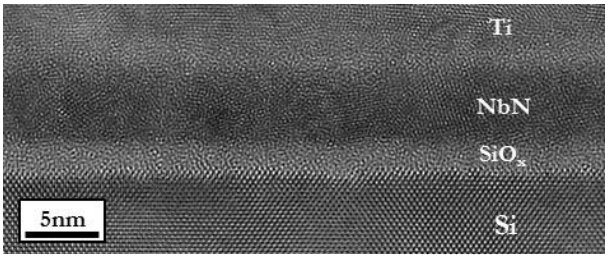

Figure 4. HRTEM image of NbN grown onto silicon with native amorphous SiO_x layer. The poly-crystalline structure is clearly pronounced as in contrast to those on AlGaN due to the large lattice-mismatch.

3.4. Critical temperature and RRR

All samples were separately mounted on a four-point-probe fixture with closely attached temperature sensor and slowly dipped into the LHe (liquid helium) Dewar. A critical temperature as high as 13.2K with narrow transition width has been attained for NbN films deposited onto the GaN buffer-layer at the substrate holder temperature of 650°C. Figure 5 summarizes the results of current and previous reported studies on commonly employed buffer-layers for the growth of NbN ultra-thin films and indicates the increase in Tc by 10% compared to MgO layers. Furthermore, NbN was simultaneously deposited at 525°C onto the GaN buffer-layer; which itself was grown both onto sapphire substrate and bare silicon. The critical temperatures reached for those films are similar and amount to 13K and 12.8K, respectively. Thus, eventual effects of the underlying sapphire substrates on the growth of NbN can be excluded and the suitability of the thin GaN epi-layer on silicon substrates has been demonstrated.

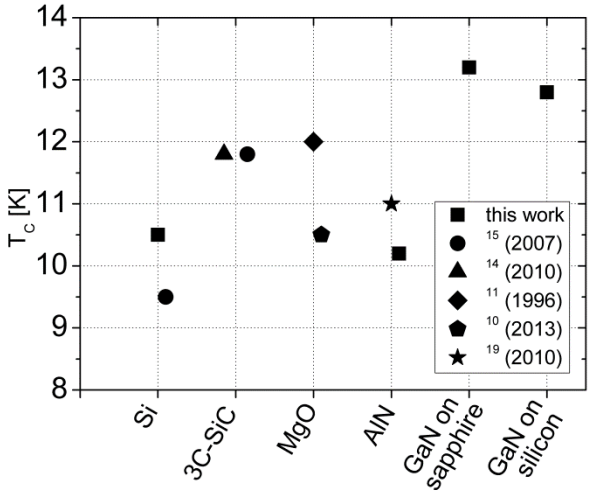

Figure 5. Current state-of-the-art NbN ultra-thin films with thicknesses ranging from 3.5 to 6nm grown on different buffer-layer.

The Al content x in the $Al_xGa_{1-x}N$ composition clearly exerts influence on NbN superconducting properties such as the gradual degradation of Tc involving a rise in R_{sheet} when increasing x above 20% as illustrated in figure 6 (a). The sheet resistance was calculated upon known sample geometry and area size [20]. Also worth noting that R_{sheet} of NbN on GaN layer is almost half of that measured for NbN deposited onto the AlN epi-layer and significantly lower than the one deposited onto bare silicon.

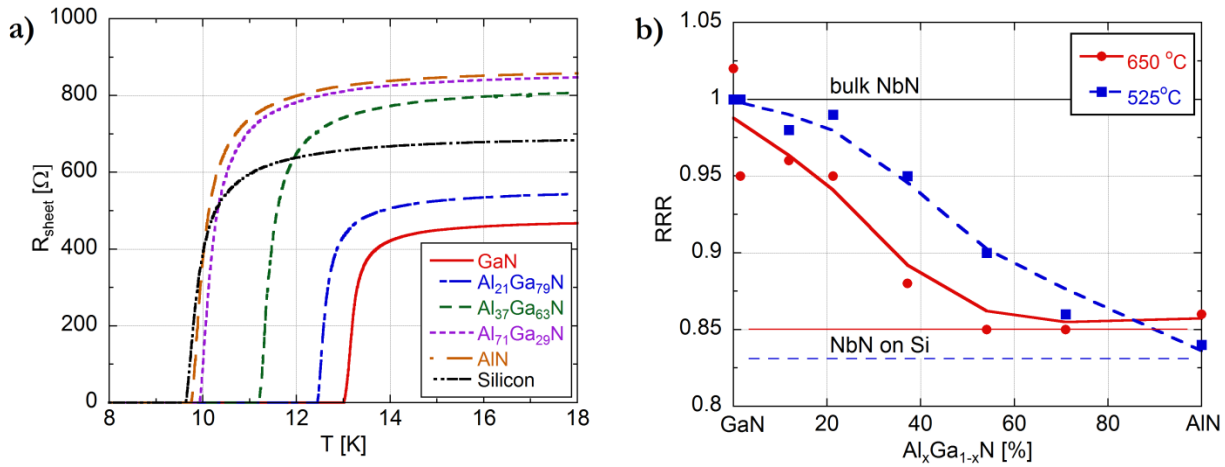

Figure 6. (a) Sheet resistance of NbN grown at 650°C onto $Al_xGa_{1-x}N$/sapphire substrates as a function of temperature for different Al content in comparison with bare silicon. (b) RRR versus Al content deposited at 525°C and 650°C, respectively.

The RRR is considered as an important figure-of-merit for providing information on structural properties such as disorder and is unity in the case of bulk NbN [21,22]. Figure 6 (b) depicts the dependence of RRR as a function of increasing Al content in comparison with silicon substrate grown at two different temperatures. The RRR close to unity for GaN epi-layers is evidence for an epitaxial growth as confirmed by HRTEM. Moreover, the RRR gradually decreases with increasing Al content and complements the deterioration of the films' Tc. The slight shift in the curves for 650°C and 525°C may be attributed to greater contamination with impurities, resulting in lower RRR due to the increased outgassing at higher substrate holder temperatures.

3.5. Film uniformity

A number of at least 10 micro-bridges with bridge dimensions ranging from 5*5µm to 4*20µm distributed across the entire wafer area were manufactured and characterized by R(T) measurements in a dedicated laboratory arrangement. It should be mentioned that all films were stored at ambient atmosphere up to one month before they were processed. Nevertheless, re-measuring of randomly chosen samples has shown that the superconducting properties such as Tc and R_{sheet} are scarcely degraded.

Table 1. Statistical summary, taken over 10 samples measured on 5nm thin NbN micro-bridges across the entire film area.

buffer-layer/ substrate	film as deposited		patterned micro-bolometers		R_{sheet} at 20K	
	Tc [K]	ΔTc [K]	Tc [K]	ΔTc [K]	[Ω]	std(R_{sheet}) [%]
GaN	13.2	1.1	12.83±0.04	1.38±0.04	492±20	4
$Al_{0.21}Ga_{0.79}N$	12.8	1.22	12.55±0.07	1.54±0.04	647±23	3.5
$Al_{0.37}Ga_{0.63}N$	12.5	1.28	12.31±0.02	1.57±0.05	587±26	4.8
$Al_{0.54}Ga_{0.46}N$	11.5	1.55	11.3±0.05	1.86±0.05	807±35	4.3
$Al_{0.71}Ga_{0.29}N$	10.2	1.73	10.0±0.12	2.02±0.07	900±81	9
Silicon	10.1	1.61	9.78±0.02	1.91±0.02	970±85	8.8

After processing, the measured Tc of the NbN films on the GaN buffer-layer remained as high as 12.83K. The standard deviation of the sheet resistance, R_{sheet} indicates homogenous films and is markedly low, from 3.5% to 4.8% for epitaxially-grown NbN film on AlGaN buffer-layer. In contrast, the corresponding standard deviation of the sheet resistance for poly-crystalline films on silicon and $Al_{>0.54}Ga_{<0.46}N$ are twice as high. The deterioration of Tc from 12.83K down to 10K and broadening of the superconducting

transition width ΔTc with increasing Al content is distinct. Moreover, the data presented in table 1 confirms high film uniformity and gives evidence that no damage has been introduced to the films due to the processing of micro-bridges.

3.6. Critical current and magnetic field measurement

Prior to preparing the samples for HRTEM, critical magnetic field and critical current measurements were carried out on NbN micro-bridges on GaN, $Al_{0.54}Ga_{0.46}N$ and silicon substrates with dimensions of 5nm*10µm*70µm in thickness, width and length, respectively. Figure 7 (a) depicts the dependence of critical current on temperature. The measured data was fitted by applying the simplified Ginzburg-Landau relationship [23] and shows satisfactory agreement. The extracted critical current density J_{c0} amounts to 3.8MA/cm^2 for NbN films deposited on GaN buffer-layer and deteriorates to 1.2MA/cm^2 for the films on bare silicon. These results agree well with other reported results on poly-crystalline films of similar thicknesses [14]. The extracted critical current density for $Al_{0.54}Ga_{0.46}N$ of J_{c0} = 2.1MA/cm^2 falls between the current density of the NbN films deposited onto the GaN buffer-layer and silicon. The critical magnetic field measurements as seen in figure 7 (b) allowed for the estimation of diffusion constants in the ultra-thin NbN film [24].

$$D = -\frac{0.407\pi k_B}{e}\left(\frac{d\mu_0 H_{c2}}{dT}\right)^{-1} \tag{1}$$

Applying the derivative of the critical magnetic field over the temperature in the vicinity of zero-field Tc0 according to (1) yielded diffusion constant on silicon substrates of approximately 0.41cm^2/s, which agrees well to the value of 0.4cm^2/s reported [25]. In contrast, the diffusion constant extracted for NbN on GaN buffer-layer is significantly enhanced and reaches 0.63cm^2/s, confirming the improved structural properties such as high order and low defect density. This can particularly be employed in utilizing an additional diffusion-cooling channel in phonon-cooled HEB mixers in order to further increase the IF bandwidth as recently demonstrated [26,27].

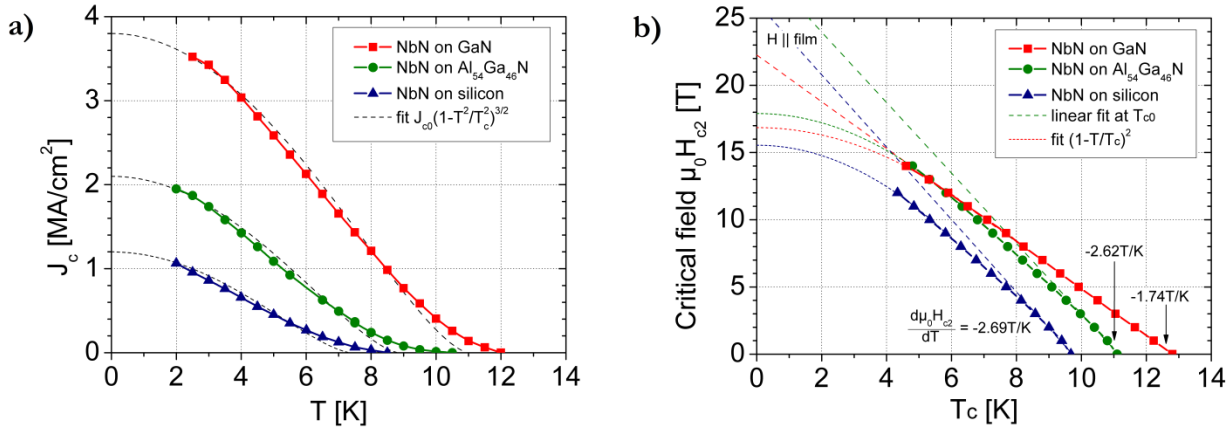

Figure 7. (a) Critical current density as a function of temperature for NbN on GaN and $Al_{0.54}Ga_{0.46}N$ substrate in comparison with silicon. The films were deposited at 625°C and micro-bridges with dimensions of 5nm*10µm*70µm fabricated. (b) Upper critical magnetic field versus Tc of GaN, $Al_{0.54}Ga_{0.46}N$ and silicon substrate with corresponding curve-fitting.

4. Conclusion

We successfully demonstrated the possibility of growing single-crystal epitaxial NbN films on $Al_xGa_{1-x}N$ (x<20%) buffer-layers by means of reactive DC magnetron sputtering. As a result, state-of-the-art ultra-thin NbN films on GaN buffer-layer with thickness of approximately 5nm and high homogeneity confirmed by HRTEM and HAADF/STEM have been deposited with Tc as high as 13.2K and RRR close to unity. Upon the fabrication of micro-bridges across the entire film area, R(T) measurements revealed high film uniformity with the standard deviation of 3.5%-4.8% of the sheet resistance for deposited NbN films onto AlGaN substrates whereas that on silicon amounted to 8%. Furthermore, the critical current density for NbN films grown onto the GaN buffer-layer is more than 3 times higher compared to silicon substrates and amounts to 3.8MA/cm^2. It has been observed that the superconducting properties gradually deteriorated when increasing the Al content of the $Al_xGa_{1-x}N$ composition above 20% and eventually approach those of films deposited onto bare silicon. The diffusion constants deduced from critical magnetic field measurements are 0.63cm^2/s of NbN on GaN buffer-layer compared to 0.41cm^2/s of NbN on silicon.

It is expected that the employment of GaN material as a buffer-layer for the deposition of ultra-thin NbN films prospectively benefit terahertz electronics, particularly hot electron bolometer (HEB) mixers.

Acknowledgement
The authors acknowledge Alexei Kalaboukhov at Quantum Device Physics Laboratory, Chalmers University of Technology, for his conducted measurements of the critical current and second critical magnetic field of the ultra-thin NbN films. The work on the employed substrates with AlGaN buffer-layer was partially supported by the NCBR in the frame of Project INNOTECH-K2/IN2/85/182066/NCBR/13, and by MRR in the frame of the Project POIG.01.01.02-00-015/09-00.

References

[1] Gershenzon E, Gol'tsman G, Gogidze I, Gusev Y, Eliantev A, Karasik B, Semenov A 1990 *Sov. Phys. Supercond.* **3**, 1582
[2] Semenov A, Hübers H-W, Schubert J, Gol'tsman G, Elantiev A, Voronov B, Gershenzon E 2000 *J. Appl. Phys.* **88**, 6758
[3] Meledin D, Pavolotsky A, Desmaris V, et al., 2009 *IEEE Trans. Microw. Theory Tech.* **57**, 89
[4] Kulesa C 2011 Terahertz Spectroscopy for Astronomy: From Comets to Cosmology *IEEE Transactions on Terahertz Science and Technology*, **1** 1
[5] Sergeev A, Reizer M 1996 Photoresponse Mechanism of Thin Superconducting Films and Superconducting Detectors *International Journal of Modern Physics B* **10** 6 635-667
[6] Il'in K, Lindgren M, Currie M, Semenov A, Gol'tsman G, Sobolewski R, Cherednichenko S, Gershenzon E 2000 Picosecond hot-electron energy relaxation in NbN superconducting photodetectors *Appl. Phys. Lett.* **76** 19
[7] Kang L, Jin B, Liu X, Jia X, Chen J 2011 Suppression of superconductivity in epitaxial NbN ultrathin films *J. Appl. Phys.* **109** 033908
[8] Cherednichenko S, Khosropanah P, Kollberg E, Kroug M, Merkel H 2002 *Physica C* **407** 372-376
[9] Gao J, Hovenier J, Yang Z, Baselmans J, Baryshev A, Hajenius M, Klapwijk T, Adam A, Klaassen T, Williams B, Kumar S, Hu Q, Reno J 2005 *Appl. Phys. Lett.* **86** 244104
[10] Kawakami A, Tanaka S, Yasui M, Hosako I, Irimajiri Y 2013 Design and Fabrication of NbN Terahertz Hot Electron Bolometer Mixers *24th International Syposium on Space Terahertz Technology*
[11] Wang Z, Kawakami A, Uzawa Y, Komiyama B 1996 Superconducting properties and crystal structures of singlecrystal niobium nitride thin films deposited at ambient substrate temperature *J. Appl. Phys.* **79** 7837
[12] Gol'tsman G et al. 2005 *Proc. SPIE* **5727** 95-106

[13] Lamaestre R, Odier P, Bellet-Amalric E, Cavalier P, Pouget S, Villégier J-C 2008 High Quality Ultrathin NbN Layers On Sapphire for Superconducting Single Photon Detectors *Journal of Physics, Conference Series* **97** 012046
[14] Dochev D, Desmaris V, Pavolotsky A, Meledin D, Lai Z, Henry A, Janzen E, Pippel E, Woltersdorf J, Belitsky V 2010 Growth and Characterization of Epitaxial Ultra-Thin NbN Films on 3C-SiC/Si substrates for Terahertz Applications *Superconductor Science and Technology* **24**
[15] Gao J, Hajenius M, Tichelaar F, Klapwijk T, Voronov B, Grishin E, Gol'tsman G, Zorman C, Mehregany M 2007 Monocrystalline NbN nanofilms on a 3C-SiC/Si substrate. *Appl. Phys. Lett.* **91**, 062504
[16] Bougrov V, Levinshtein M, Rumyantsev S, Zubrilov A 2001 Properties of Advanced Semiconductor Materials GaN, AlN, InN, BN, SiC, SiGe. *John Wiley & Sons, Inc. New York* 1-30
[17] Li X, Yang R 2012 Effect of lattice mismatch on phonon transmission and interface thermal conductance across dissimilar material interfaces *Physical Review B* **86** 054305
[18] Edgar J, Du L, Lee R, Nyakiti L, Chaudhuri J 2008 Native oxide and hydroxides and their implication for bulk AlN crystal growth *Journal of Crystal Growth* **310** 4002
[19] Shiino T, Shiba S, Sakai N, Yamakura T, Jiang L, Uzawa Y, Maezawa H, Yamamoto S 2010 *Superconductor Science and Technology* **23** 045004
[20] Smits F 1958 Measurement of Sheet Resistivities with the Four-Point Probe *BSTJ* **37** 711
[21] Jones H 1975 *Appl. Phys. Lett.* **27** 471
[22] Marsili F, Bitauld D, Fiore A, Gaggero A, Mattioli F, Leoni R, Benkahoul M, Levy F 2008 *Opt. Express* **16** 3191
[23] Cyrot M 1973 Ginzburg-Landau theory for superconductors *Rep. Prog. Phys.* **36** 103
[24] Martins B 2006 New Frontiers in Superconductivity Research *Nova Science Publishers, New York* 171
[25] Floet D, Gao J, Klapwijk T, Korte P 2001 Thermal time constant of Nb diffusion-cooled superconducting hot-electron bolometer mixers *IEEE Trans. Appl. Supercond.* **11** 187-190
[26] Ryabchun S, Tretyakov I, Finkel M, Maslennikov S, Kaurova N, Seleznev V, Voronov B, Gol'tsman G 2008 Fabrication and characterization of NbN HEB mixers with in situ gold contacts *19th International Symposium on Space Terahertz Technology*
[27] Finkel M, Vachtomin Y, Antipov S, Drakinski V, Kaurova N, Voronov B, Gol'tsman G 2003 Gain Bandwidth and Noise Temperature of NbTiN HEB Mixers *14th International Symposium on Space Terahertz Technology*